

Regional fracture patterns around volcanoes: Possible evidence for volcanic spreading on Venus

I. López^{a,*}, J. Lillo^a, V.L. Hansen^b

^a *Área de Geología, Escuela Superior de Ciencias Experimentales y Tecnología, Departamental I-Despacho 211, Universidad Rey Juan Carlos, 28933, Móstoles, Madrid, Spain*

^b *Department of Geological Sciences, University of Minnesota–Duluth, Duluth, MN 55812, USA*

Received 26 July 2005; revised 19 December 2007

Available online 5 February 2008

Abstract

Magellan data show that the surface of Venus is dominated by volcanic landforms including large flow fields and a wide range of volcanic edifices that occur in different magmatic and tectonic environments. This study presents the results from a comprehensive survey of volcano–rift interaction in the BAT region and its surroundings. We carried out structural mapping of examples where interaction between volcanoes and regional fractures results in a deflection of the fractures around the volcanic features and discuss the nature of the local volcano-related stress fields that might be responsible for the observed variations of the regional fracture systems. We propose that the deflection of the regional fractures around these venusian volcanoes might be related to volcanic spreading, a process recognized as of great importance in the tectonic evolution of volcanoes on Earth and Mars, but not previously described on Venus.

© 2008 Elsevier Inc. All rights reserved.

Keywords: Venus, surface; Volcanism; Tectonics

1. Introduction

Magellan data show that the surface of Venus is dominated by volcanic landforms including large flow fields and a wide range of volcanic edifices that occur in different magmatic and tectonic environments (e.g. Head et al., 1992; Guest et al., 1992; Crumpler et al., 1997; Crumpler and Aubele, 2000). There are over 1700 magmatic centers larger than 20 km in diameter scattered across the surface; one region, Beta-Atla-Themis (BAT), shows several times the global average density of volcanic edifices (Crumpler et al., 1993, 1997; Crumpler and Aubele, 2000). Venusian volcanoes are divided into three classes (e.g. Barsukov et al., 1986; Crumpler et al., 1997) based on diameter (central edifice and surrounding flow apron): (1) large volcanoes (≥ 100 km); (2) intermediate volcanoes (≥ 20 and < 100 km); and (3) small volcanoes (< 20 km). Steep-sided

domes and modified or fluted volcanoes are mainly ascribed to the intermediate volcano class (e.g. Pavri et al., 1992; Bulmer and Guest, 1996).

The study of volcano–rift interactions on Earth and Mars reveals that the fracture patterns around volcanoes located in extensional settings (i.e. rifts) result from the interaction between the regional tensional stress fields and local volcano-related stress fields, and could reflect aspects of the subvolcanic rheological profile (e.g. van Wyk de Vries and Merle, 1996; van Wyk de Vries and Matela, 1998; Mège et al., 2003). Therefore, analysis of such fracture patterns can place constraints on the deformation style and the stress state of the volcano, and, as such, might allow preliminary predictions about the basement configuration, or rheology.

Despite similarities in size and composition, Venus and Earth evolved along different tectonic pathways: Earth developed a full system of moving plates, whereas Venus represents a ‘one plate planet.’ As a consequence, the regional and local effects of tectonic and magmatic activity on Venus might best be defined as ‘intraplate.’ A key assumption in the interpretation of the Venus’ geologic record is that liquid water has not played

* Corresponding author.

E-mail addresses: ivan.lopez@urjc.es (I. López), javier.lillo@urjc.es (J. Lillo), vhansen@d.umn.edu (V.L. Hansen).

a significant role in the shaping of its surface. Primary evidence for this view is rooted in the extremely dehydrated state of the (current) lower atmosphere (Donahue et al., 1997) and the present surface temperature of $\sim 460^\circ\text{C}$ (Crisp and Titov, 1997). This lack of water renders surface material, presumed to be basaltic in composition (e.g. Grimm and Hess, 1997), significantly stronger than terrestrial counter parts (Mackwell et al., 1998). Thus, in addition to the absence of tectonic overprinting induced by moving plates, the lack of surface water (and hence of erosional processes; Campbell et al., 1997) has resulted in the preservation of a rich and complex history of the deformation on the surface, which facilitates the study of primary surface structures related to tectonomagmatic processes (e.g. Ernst and Desnoyers, 2004). This makes Venus a singular natural geodynamic laboratory in which to examine volcanotectonic processes and resulting fracture patterns; however, such a laboratory does not come with serious cautions for establishing local geologic histories. For example, the absence of erosion (and deposition) means that surfaces can appear ‘pristine,’ lacking aspects of degradation, and thus a proxy for time, which we have come to take for granted on Earth. The absence of erosion (or related deposition) means that events that occurred at different times might overprint one another with little direct means to differentiate the effects of possible (unrelated?) events.

This study presents the results from a comprehensive survey of volcano–rift interaction in the BAT region and its surroundings. We highlight examples where the interaction between volcanoes and regional fractures results in a deflection of the fractures around the volcanic features (e.g. large volcanoes, steep-sided domes and modified domes) and compare them with similar volcano-related fracture patterns on Earth and Mars. We also discuss the possible nature of low-strength materials (i.e. thin ductile layer) that could favor the occurrence of volcanic spreading. We further discuss the potential role that volcanic spreading might play in the modification of intermediate volcanoes on Venus.

2. Data and methodology

To study the process of volcano–rift interaction in the BAT region and its surroundings we use as a base the Magellan Venus Volcanic Feature database compiled by Crumpler and Aubele (2000) completed with data from the regularly updated Gazetteer of Planetary Nomenclature (<http://planetarynames.wr.usgs.gov/>); in addition we use full-resolution Magellan synthetic aperture radar (SAR) images of individual features. This study of the BAT region and its surroundings revealed ~ 100 examples of volcano–rift interaction; volcanoes variably predate, postdate and interact with (presumably formed synchronously with) regional fracture suites. We present here five examples in which regional fractures and volcanoes interact; in each case the interaction resulted in local modification of the regional fracture trends around the volcanic constructs (Fig. 1). These volcanic features include large volcanoes and intermediate volcanoes of different types (e.g. steep-side domes and modified or fluted volcanoes). Unnamed features are cited using the nomenclature system developed by Crumpler and Aubele (2000), that is, use

of the latitude and longitude coordinates of the volcanic feature (e.g. 10n230) together with an abbreviated identification of the type of volcanic edifice: large volcano (LV), intermediate volcano (IV), steep side dome (SSD), fluted or modified dome (FD).

Structural and geologic mapping of selected examples was carried out using NASA’s Magellan S-band (12.6 cm wavelength) synthetic aperture radar (SAR) and altimetry data (e.g. Ford et al., 1993). Data used for the study include: (1) right and left-illuminated full resolution (FMAP; 75–100 m/pixel) SAR images; (2) Magellan altimetry (~ 8 km along-track by 20 km across-track with ~ 30 -m average vertical accuracy that improves to ~ 10 m in smooth areas; Ford et al., 1993); and (3) synthetic stereo images constructed following the method of Kirk et al. (1992) using NIH-Image macros developed by Duncan Young. All SAR images were obtained through the USGS Map-a-Planet website, and all were viewed in both normal and inverted (negative) modes. Inverted images are particularly useful for structural mapping.

3. Cases studied

3.1. Ne Ngam Mons and Ajina Fossae

Ne Ngam Mons (lat. 43° S, long. 258° E; Figs. 1, 2 and 3), an ~ 220 km diameter volcano, lies in northern Helen Planitia. The main topographic edifice has a diameter of about 25 km and an altitude of ~ 400 m above its base (Fig. 3b). This main edifice has slopes of 0.6 – 0.7° and is surrounded by an outer lava apron extending up to 180 km with slopes that are about 0.08 – 0.3° . This topographic shape, similar to other large volcanoes on Venus (Keddie and Head, 1995; McGovern and Solomon, 1997; Stofan et al., 2001), has been interpreted as the result of complex eruptive histories involving frequent, low-effusion rate, summit eruptions accompanied by less frequent but voluminous flank eruptions (e.g. Stofan et al., 2001).

The main edifice, slightly elongated along a north–south trend, displays a simple circular caldera (Figs. 3c and 3d). Inside the caldera a small cone or dome (not resolved with altimetry data, but apparent in SAR) likely represents resurgent volcanic activity restricted to the summit (Fig. 3d).

Radially distributed flows of Ne Ngam Mons cover 360° of azimuth. Although these flows extend far beyond the main edifice, the age and the duration of individual flows cannot be robustly constrained, although local relative temporal relations between flows can be determined. Older flows form long bright-to-intermediate sheet flows that mark the outer limits of the volcano; inward from the flow front these flows locally outcrop as kipukas. Locally these flows fill the inner low of an unnamed corona (lat. 42° S, long. 256.6° E) to the northwest (Figs. 2 and 3a). Two small steep-sided domes, located on the corona annulus, are embayed by the Ne Ngam Mons sheet flows (Fig. 2). Other flows, that form the volcano apron, comprise younger digitate flows that display lower reflectivity values and smoother surfaces compared with former long flows that mark the perimeter of the volcano. The younger flows also display weakly defined interior flow fronts, relations inter-

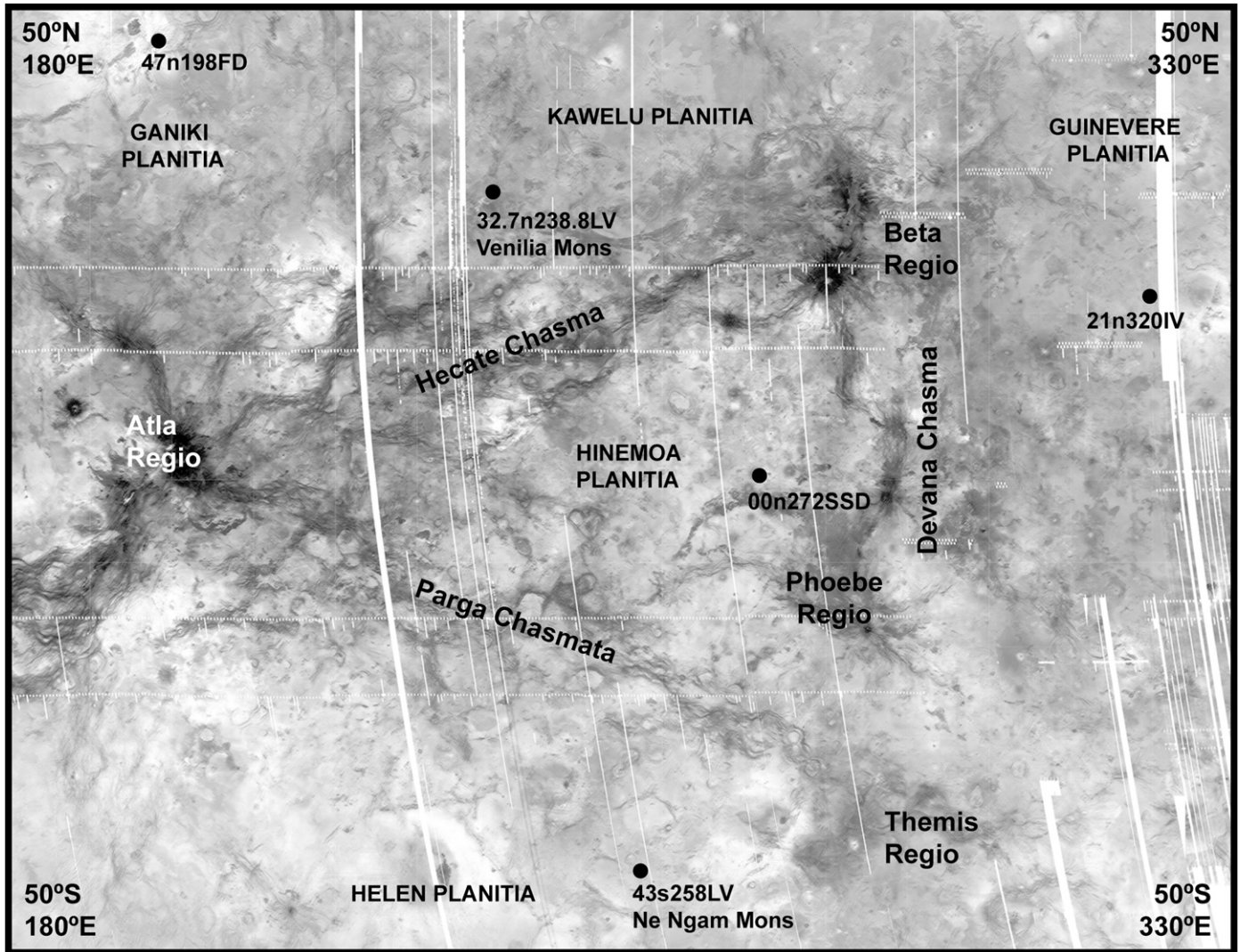


Fig. 1. SAR image of the Beta-Atla-Themis region annotated with regional locations, and the locations of the volcano–rift interaction examples discussed herein.

preted in other venusian volcanoes (e.g. Sif Mons) as evidence of broad overlapping flows (Stofan et al., 2001). Two small radar-dark elongated depressions interpreted as collapsed tubes or channels, with details below SAR resolution, cut the digitate flows along the eastern flank indicating that at least some of these flows form channel- or tube-fed flows (Figs. 3a and 3c). These primary structures, traceable for ~ 50 km, show a relatively constant width (< 2 km) and sinuous trace.

Local strain features in the main volcanic edifice include: radial fractures that extend from the summit to the base of the main edifice, and a ridge located at the base of the western flank (Figs. 3c and 3d). The radial fractures are located in the eastern flank of the main edifice and do not extend into the volcano apron. There are no flows at the terminations of the fractures, or pit chains or individual small shields associated with these fractures that might clearly indicate the existence of feeding dikes (e.g. Grosfils and Head, 1994a) under this set of late radial fractures located in the upper part of the main edifice (Figs. 3c and 3d). However Grindrod et al. (2005) note suites of radial graben and fractures, which are likely underlain by

dikes, yet which show no associated surface flows; therefore, the absence of surface flows cannot provide robust evidence to completely rule out the presence of dikes under Ne Ngam radial fractures. Other radial fractures that might indicate a previous stage of radial injections, and that might be partially or totally covered by younger materials, are not observed in the volcano surroundings. The materials on the western flank produce high radar return (i.e. backscatter) indicating high roughness; however, there is no evidence of radial fractures (Fig. 3c).

A NNW-SSE trending concentric ridge lies along the western base of the main edifice. This structure is interpreted to record local contraction restricted to the western base of the main edifice; the nearest suite of regional contractional features are NW-SE trending wrinkles ridges of the Helen Planitia-trend (Billoti and Suppe, 1999) located ~ 500 km to the southwest of Ne Ngam Mons (Fig. 3b).

The central area of Ne Ngam Mons shows a horseshoe-shaped morphology that opens to the west, with the main volcanic edifice located inside the horseshoe topography (Figs. 3a and 3b). The horseshoe-shaped morphology is not, however, ap-

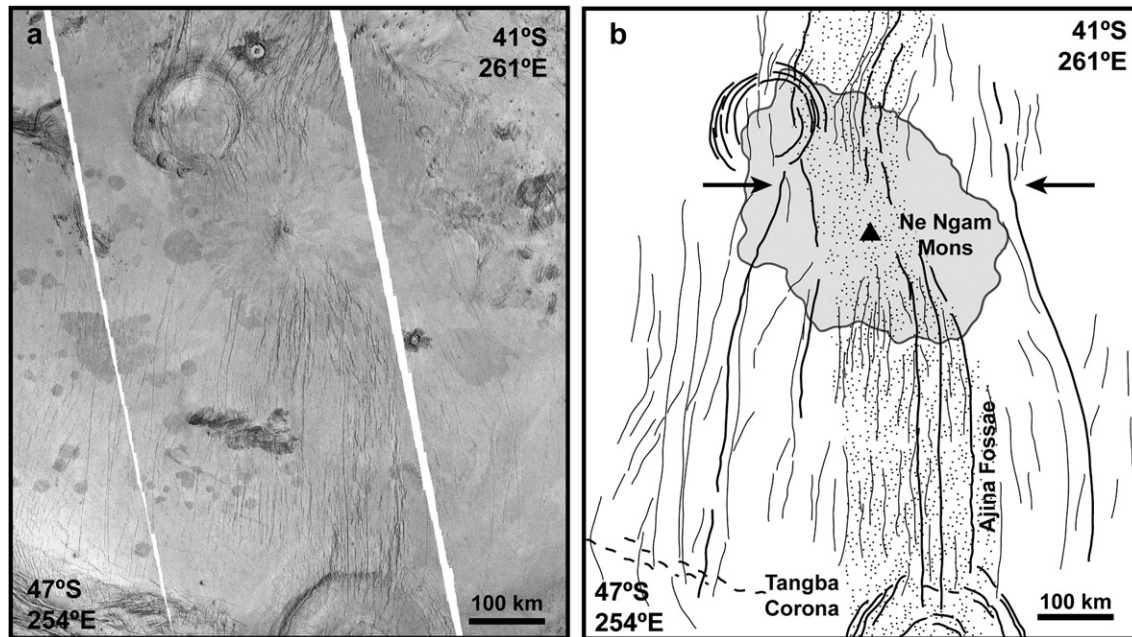


Fig. 2. (a) Mercator projection of left-illumination inverted SAR image of Ne Ngam Mons and Ajina Fossae. (b) Structural sketch map of the region shown in (a), illustrating the principal regional fractures. The triangle marks the location of the volcano main edifice. Bold lines and arrows mark regional fractures that bend toward the volcano. The stipple pattern marks the inner portion of the fracture belt that connects Tangba Corona and Ne Ngam Mons, and that is captured by the volcano. Dashed lines represent regional wrinkle ridges.

parent in the SAR data, a data set that is sensitive to topography. On Earth, horseshoe-shaped or amphitheatre morphologies in volcanic edifices provide evidence for the occurrence of lateral flank collapse processes (e.g. Socompa volcano, Chile; Francis et al., 1985). Given that the horseshoe-shaped morphology cannot be confirmed in the case of Ne Ngam Mons, the occurrence of collapse processes remains unconfirmed. In addition, Ne Ngam Mons lacks obvious collapse-associated deposits (i.e. hummocky terrain; Siebert, 1984). If collapse occurred on Ne Ngam Mons, it occurred during a previous stage of evolution with the present main edifice located inside the collapse-related amphitheatre (e.g. Kick'em Jenny submarine volcano in the Antilles Volcanic Arc; Watlington et al., 2002) with flows overprinting the collapse-related materials. However, flows of Ne Ngam Mons do not appear to have been influenced by previous topography; flows radiate around the volcano without apparent modification of the flow morphology. This suggests that the horseshoe morphology could be an artifact of the topographic data, rather than true morphology related to volcano evolution.

Ne Ngam Mons occurs in spatial association with a 150-km wide and 300-km long north-trending fracture system, Ajina Fossae (lat. 45° S, long. 258° E). Ajina Fossae, which parallels a regionally distributed north-trending fracture suite that dominates northern Helen Planitia, consists of: (a) an inner section, with close inter-fracture spacing, that connects Ne Ngam Mons and Tangba Corona (lat. 47° S, long. 258° E; stipple pattern in Fig. 2); and (b) an outer section, marked by more widely-spaced fractures that gradually merge with the regionally distributed north-trending fracture suite.

The formation of Ne Ngam Mons and Ajina Fossae are temporally related. The oldest and longest flows of Ne Ngam Mons

predate the north-striking fractures of Ajina Fossae, which are, in turn, covered by late digitate flows. Interaction between the volcano and the fracture zone occurs in two ways (Fig. 2): (a) north-striking fractures that form the central part of Ajina Fossae (stipple pattern in Fig. 2b) bend toward the main edifice of the volcano, producing a deviation (i.e. capturing) of the fracture belt; and (b) north-striking fractures located in the outer part of the fracture system bend toward the volcano in a characteristic hourglass pattern. In both cases the modification in the trend of the fractures varies $\sim 20^\circ$.

3.2. Venilia Mons and Arianrod Fossae

Venilia Mons (lat. 32.7° N, long. 238.8° E) is a 320 km diameter large shield volcano located in western Kawelu Planitia (Fig. 1). Venilia Mons consists of a central edifice (200 m of height above its base, 35 km diameter) and a flow apron that extends up to 320 km in diameter radial to the central edifice (Fig. 4). A gradual topographic transition marks the boundary between the main edifice and the flow apron. Locally individual pits occur at the summit of Venilia Mons, which generally lacks primary or secondary summit structures. There are no radial fractures and/or pit chains that might mark the surface expression of a system of underlying radial dikes. Although other features, such as individual pits and small edifices, could indicate the presence of radial dikes, none are clearly defined. In some volcanic features proximal flows in the volcano flanks postdate, and thus cover radial fractures; however, in such cases evidences of subsurface transport is observed far from the center of the edifice (e.g. Ernst et al., 1995). This situation is not observed in Venilia Mons. Radially distributed flows of varied backscatter, length and morphology extend beyond the main ed-

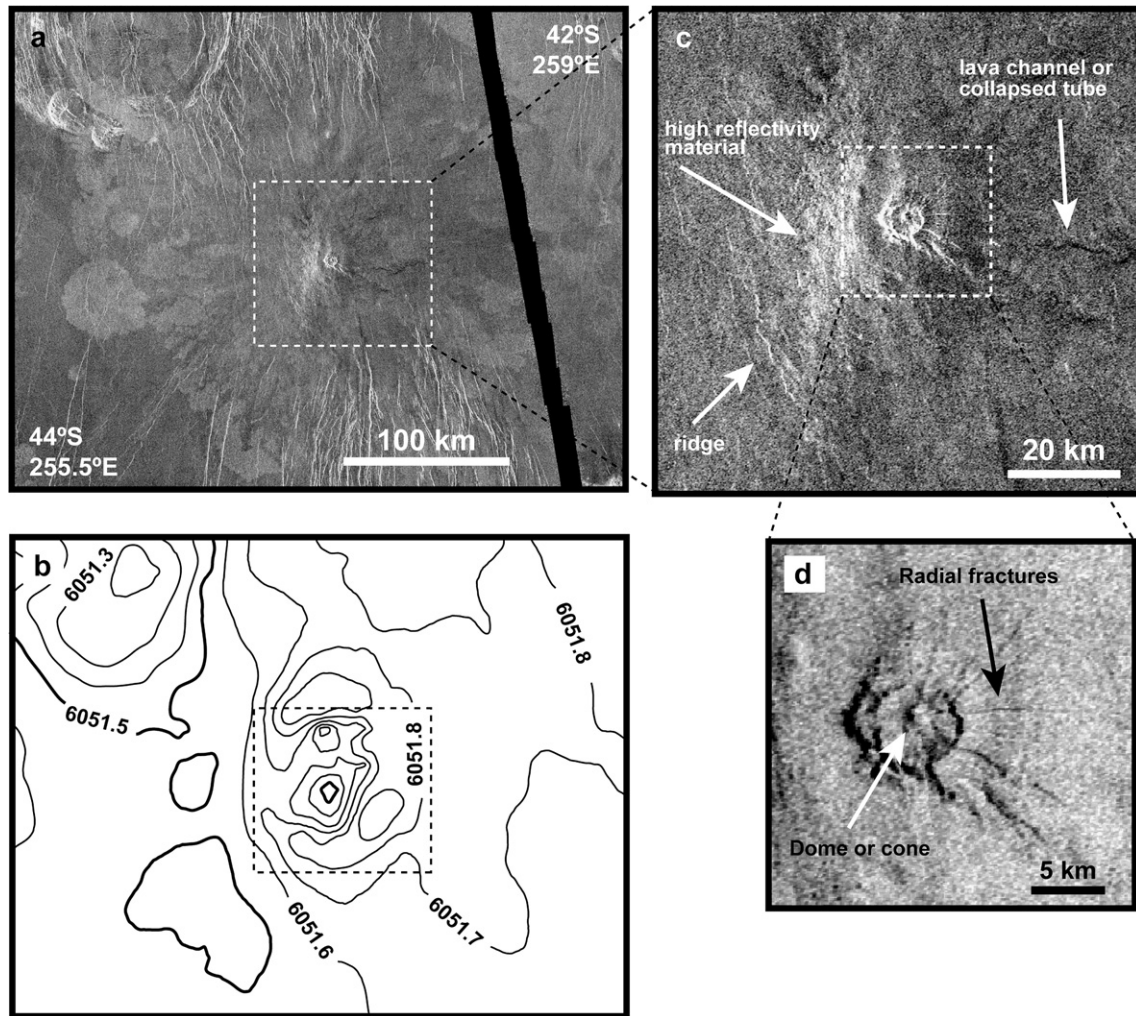


Fig. 3. (a) Mercator projection of left-illumination normal SAR image of the main edifice and radial flows of Ne Ngam Mons (lat. 43° S, long. 258° E); rectangle indicates location of (c). (b) Topographic map of the region shown in (a) (100 m contour interval; topography data from Ford and Pettengill, 1992); rectangle indicates location of (c). (c) Mercator projection of left-illumination normal SAR image of the main edifice of Ne Ngam Mons; square indicates location of (d). (d) Detail of radial fractures on Ne Ngam Mons main edifice (left-illumination inverted SAR image).

ifice of Venilia Mons (Fig. 4). The flow apron displays weakly defined interior boundaries and multiple overlapping sheets. We cannot constrain the relative age of individual flows, or the duration of Venilia Mons formation.

Venilia Mons is spatially associated with Arianrod Fossae (lat. 37° N, long. 239.9° E), a NE-trending 715-km long regional fracture system composed of fractures and graben. Fractures of Arianrod Fossae postdate some radial flows of Venilia Mons but these fractures are in turn covered by other volcano-related flows (Fig. 4). This observation suggests a temporal relation between the formation of the volcano and the fracture system. Most of the flows originate from the volcano although some of the flows, located to the south of Venilia Mons, could result from fissure eruptions related to Arianrod Fossae. Many small shields that locally postdate both the regional fractures and the volcano-related flows surround Venilia Mons. Other evidence for temporal relations between the formation of Arianrod Fossae and Venilia Mons is that NE-SW trending regional fractures of the fracture system curve toward the volcano, suggesting a local modification in the regional-fracture trend re-

lated to local volcano-related stress fields. This modification in the trend of the regional fractures varies between 20° and 40° (Fig. 4b).

3.3. 47n198FD

47n198FD (Fig. 5), an unnamed intermediate-size modified or fluted dome lies northeast of Nemesis Tessera between Vinmara Planitia and Ganiki Planitia (Fig. 1). 47n198FD is a 25-km diameter volcanic edifice with a height of 200 m above its surrounding terrain; it was not identified in the volcanic feature database of Crumpler and Aubele (2000). The original characteristics and topographic shape of the volcano are difficult to constrain due to post-formation modification and volcanic embayment (Fig. 5c). The volcano displays a fractured summit with several circular scarps that might result from multiple caldera collapses events during volcano evolution (Fig. 5c). The volcano surroundings lack radial fractures, which might represent surface evidence of a dike system associated with 47n198FD. Many pits and small shield volcanoes, located in

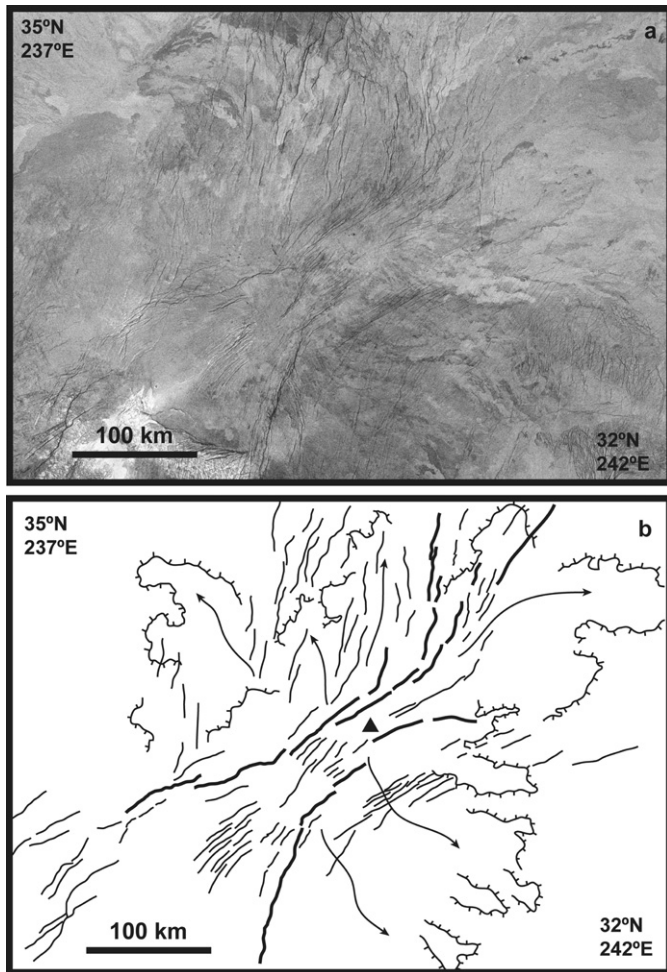


Fig. 4. (a) Mercator projection of left-illumination inverted SAR image of Venilia Mons and Arianrod Fossae. (b) Structural sketch map of the region shown in (a), illustrating the principal regional fractures (bold lines). The triangle marks the volcano main edifice. Principal regional fractures bend toward the volcano; arrows and lobate fronts mark the direction and extent of the volcano flows.

the area surrounding the volcano, postdate the formation of regional fractures and 47n198FD, and could represent evidence of volcano-associated dikes (Fig. 5c). However, the presence of pits and shields dispersed well beyond the area surrounding the volcano might also indicate that these primary features are of regional origin, rather than genetically associated with the volcano. Due to their point-sourced nature, shields can result in local burial of earlier-formed volcano-related features and therefore hamper analysis. 47n198FD lacks a radial flow apron, although local point-source shield volcanic or regional volcanic materials could cover earlier formed flows. Flows could have also been homogenized (with respect to backscatter) due to weathering processes (Arvidson et al., 1992), and, as such they cannot be differentiated from the surrounding materials.

47n198FD occurs within an ~ 1000 km long suite of NE-trending regional fractures that extend between Vinmara Planitia and Ganiki Planitia. Formation of 47n198FD and the regional fractures overlapped in time: the volcanic feature post-dates formation of some regional fractures but volcanic materi-

als that embay 47n198FD are in turn cut by fractures (Fig. 5c). Interaction between regional fractures and the volcano can also be interpreted based on the deflection of some regional fractures in the vicinity of the volcano. Regional fractures bend toward the volcano in a characteristic hourglass pattern (Fig. 5); near the volcano fractures display a $\sim 10^\circ$ angular deviation from the regional NE trend.

3.4. 00n272SSD

00n272SSD, an elliptical steep-sided dome (20×15 km) with a height of ~ 200 m above its base, lies in eastern Hinemoa Planitia just north of Phoebe Regio (Figs. 1 and 6). This steep-sided dome, large enough (≥ 20 km) to be considered an intermediate volcanic feature, is not included in the volcanic features database of Crumpler and Aubele (2000). 00n272SSD has an irregular summit with NW-trending graben and fractures; it lacks evidence of vents or collapse pits (Fig. 6c). Steep slopes mark the north–northwest side, whereas a more gradual slope marks the transition to the plains to the southeast. No scarps or debris apron, related to modification processes, are observed. 00n272SSD-related flows occur to the north (Fig. 6c). These ~ 15 -km long flows display simple lobate morphology, and backscatter similar to that of the surrounding plains. Along the south base of the dome, fractures could both pre-date dome-related flows or small shield volcanoes and associated materials, and post-date dome-related flows. Even in the highest resolution SAR images we observe no evidence of radial fractures, pit chains or radially arranged smaller volcanic features—any or all of which might indicate the presences of a system of radial dikes associated with the volcano.

00n272SSD interacts with a set of NE-trending regional fractures and graben (Fig. 6). The dome and fractures formed contemporaneously; the dome covers regional fractures that in turn cut dome-related flows to the north. Some regional fractures modify their trend in the vicinity of 00n272SSD and bend toward the volcanic construct, deviating $\sim 10^\circ$ (Fig. 6).

3.5. 21n320IV

21n320IV, a 25–40 km intermediate-size volcanic feature, lies in southern Guinevere Planitia just north of Lauffey Regio (Figs. 1 and 7). The volcanic edifice is delimited by a set of concentric fractures and west–northwest facing scarps with a small conical volcano (< 10 km), which could represent resurgent activity (Fig. 7c). 21n320IV lacks clear lobate flows, although some materials that cover regional fractures to the northwest could have their origin in the volcanic edifice (Fig. 7c). Small shield volcanoes and related materials partially cover the regional fractures and might also mask volcano-related flows. Local strain features in 21n320IV include concentric fractures and scarps that delimit the extent of the volcanic edifice (Fig. 7c). We do not observe a radial system of fractures centered in the volcanic feature that could be related to the existence of dikes. If such a system once existed, it is completely covered by flows of the volcanic edifice, regional volcanic materials, and/or shield-related volcanic material.

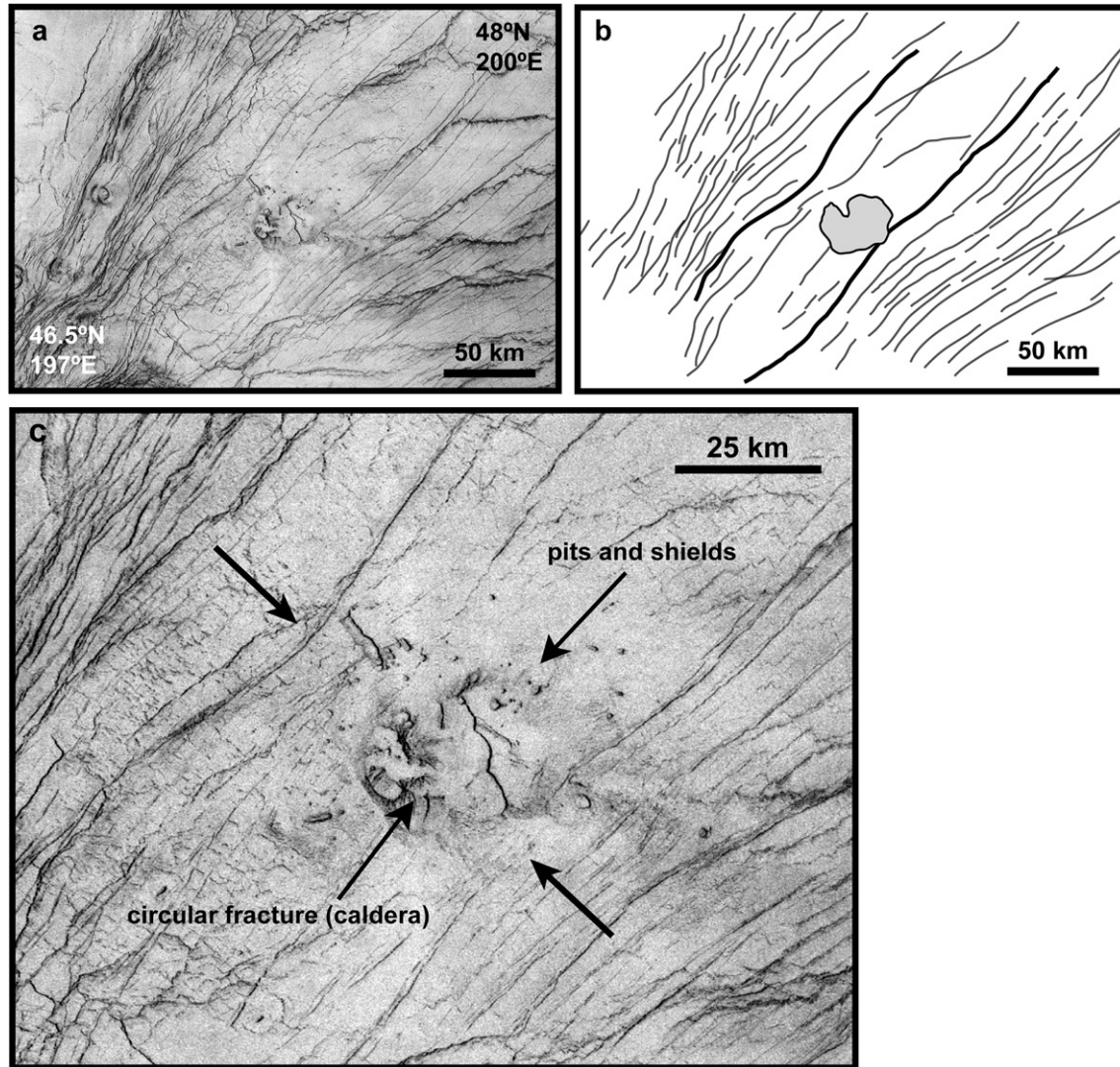


Fig. 5. (a) Mercator projection of left-illumination inverted SAR image of 47n198FD. (b) Structural sketch map of the region shown in (a); bold lines mark principal regional fractures; the gray area defines the volcanic edifice. (c) Left-illumination inverted SAR image of the volcano edifice. Arrows mark examples of regional fractures with a modified trend around the volcanic edifice and the location of pits and shields in the volcano area.

21n320IV lies within a regional NW-trending suite of fractures and graben. Fracture trend is locally modified in the vicinity of the volcanic edifice with fractures curving around the volcanic feature (i.e. wristwatch morphology; Fig. 7c). We cannot determine if the formation of the volcano is temporally related to fracture formation (i.e. local modifications of the fracture patterns due to volcano-related local stress fields) or if the fractures formed later due to deformation partitioning around the volcano.

4. Fracture patterns around volcanoes on terrestrial planets

Local volcano-related stress regimes can interact with regional stress regimes resulting in a variety of fracture patterns around volcanic structures. Studies on Earth, Mars and Venus lead workers to propose two common, but different, processes that can lead to modifications of regional fracture trends around volcanoes: (a) localization of stress fields re-

lated to over-pressurized magma chambers and formation of radial dike systems (e.g. Odé, 1957; Muller and Pollard, 1977; Chadwick and Howard, 1991; McKenzie et al., 1992; Grosfils and Head, 1994b); and (b) localization of volcano-related gravitational stresses (e.g. Cyr and Melosh, 1993; van Wyk de Vries and Merle, 1996).

4.1. Regional fracture systems and over-pressurized magma chambers

Local stress fields related magma reservoirs and dike emplacement can affect venusian rift systems (i.e. chasmata and fossae) and regionally distributed fractures (McKenzie et al., 1992). These authors propose that when the area below a volcanic edifice is depressed, subcircular dikes form causing regional fractures to curve around the volcano (Fig. 9a in McKenzie et al., 1992); in contrast, an over-pressurized magma chamber that elevates the area above the surrounding plains,

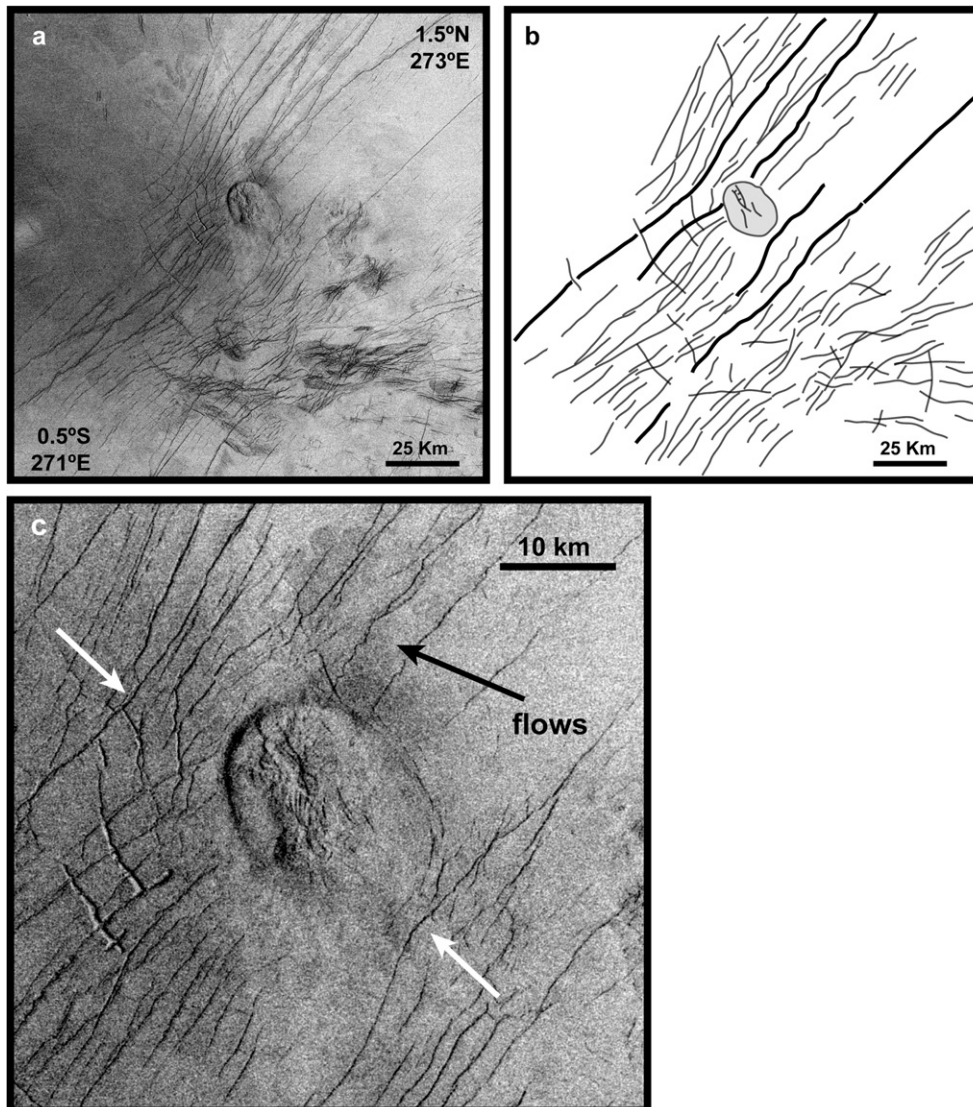


Fig. 6. (a) Mercator projection of left-illumination inverted SAR image of 00n272SSD. (b) Structural sketch map of the region shown in (a); bold lines mark principal regional fractures; the gray area marks the location of the dome. (c) Left-illumination inverted SAR image of the dome; arrows mark examples of regional fractures with a modified trend around the volcanic edifice and shield-related flows.

leads to the formation of radial dikes (Fig. 9b in McKenzie et al., 1992).

Interaction of a local stress field related to over-pressurization and dike emplacement with a regional tensional stress field leads to a concentration of strain and to a variation of the regional fracture patterns in which fractures bend toward the volcanic feature. Cyr and Melosh (1993) explained a similar deviation of regional fractures around coronae resulting from uplift and regional extension without concurrent dike emplacement. Examples of this interaction have been proposed to occur in Tempe Fossae in Mars and some segments of the North Atlantic mid-ocean ridge on Earth (e.g. Fig. 11 of Mège et al., 2003).

4.2. Local volcano-related gravitational stresses and regional fracture systems

In the case of rift-zone related volcanoes, local stress fields associated with loading, lithospheric flexure and spreading

interplay with the regional stress field, resulting in a combined stress regime that leads to a change in orientation of regional fractures near volcanoes (e.g. Cyr and Melosh, 1993; van Wyk de Vries and Merle, 1996). The result of this stress field interaction depends on the orientation and magnitude of both stress fields, as well as the rheological configuration of the basement (van Wyk de Vries and Merle, 1996; van Wyk de Vries and Matela, 1998). Volcano-related lithospheric flexure over a thick ductile basement results in (Fig. 8a): (a) compression in the center of the volcano; and (b) tension at the base of the volcano (e.g. Cyr and Melosh, 1993). In extensional fracture systems, volcanoes that load and flex the lithosphere produce stresses that result in a deviation of the regional fractures around the volcano in a characteristic ‘wristwatch’ pattern (e.g. Fantale volcano in the East African Rift System; van Wyk de Vries and Matela, 1998; Fig. 8c). Deviation of regional fractures due to the combined effect of loading and regional extension has been described around Alba Patera, Mars (e.g. Turtle and Melosh,

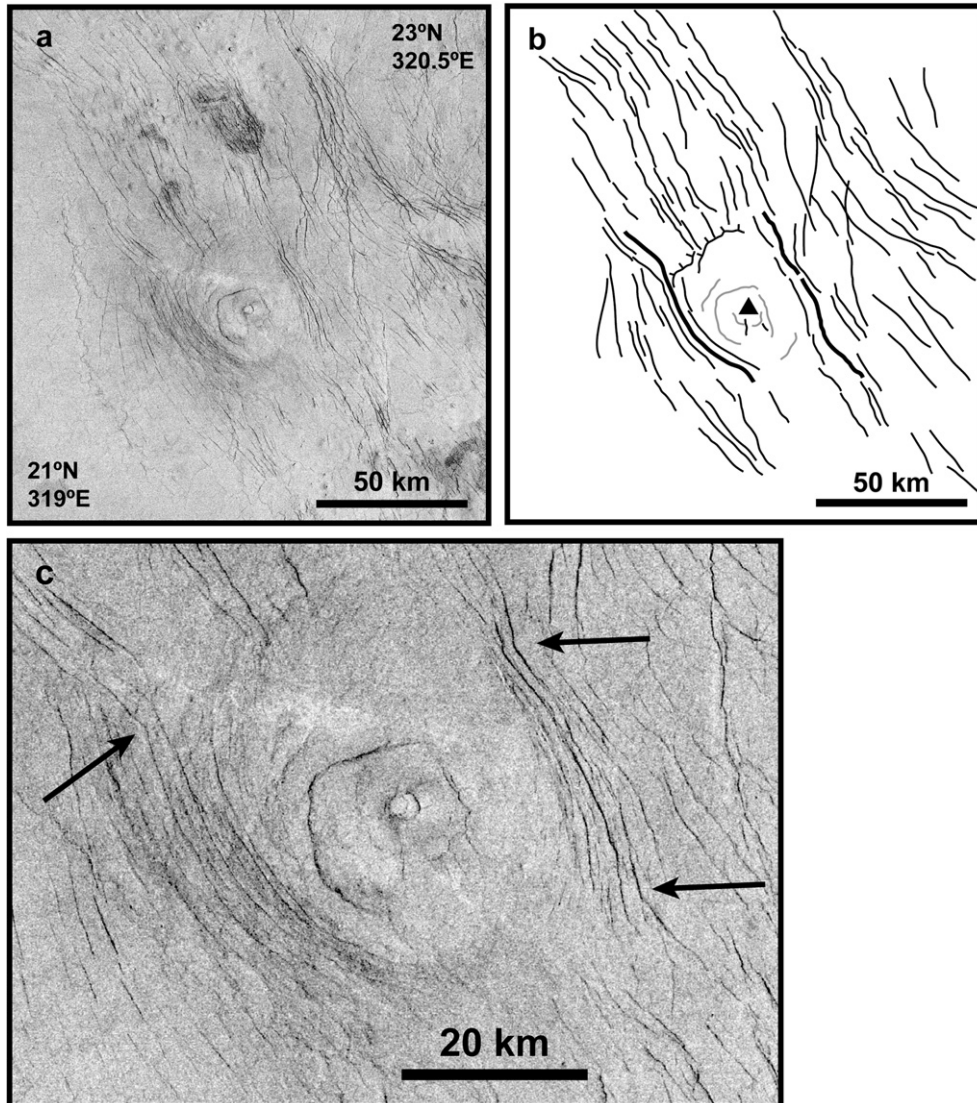


Fig. 7. (a) Mercator projection of left-illumination inverted SAR image of 21n320IV. (b) Structural sketch map of the region shown in a; the triangle marks the center of the volcanic edifice and a small resurgent volcano; bold lines mark principal regional fractures. (c) Left-illumination inverted SAR image of the volcanic edifice; arrows mark regional fractures with a modified trend around the volcanic edifice.

1997; McGovern et al., 2001) and around some venusian coronae (Cyr and Melosh, 1993).

Another situation that can cause local volcano-related stress-fields is volcanic spreading. Volcanic spreading produces a horizontal outward displacement on the slopes and peripheries of volcanoes and in the nearby substrate (e.g. Borgia et al., 2000). Associated local stress fields include: (a) tension in the volcano summit (i.e. development of radial fractures and graben), and (b) compressive stress in the main edifice base (Fig. 8b; Borgia, 1994). Volcanic spreading is favored by the presence of a thin ductile layer under the volcano that will deform and spread outward under the volcanic load (Borgia, 1994). Alternatively, a detachment rooted in a fault-like surface enables spreading, as at the Hawaiian volcanoes and perhaps Olympus Mons on Mars (e.g. Dieterich, 1988; McGovern and Solomon, 1993; Iverson, 1995).

Experimental analog models on the interaction between spreading volcanoes and rift systems and comparison with natural examples were carried out by van Wyk de Vries and Merle (1996). In these experiments (Fig. 3 of van Wyk de Vries and Merle, 1996), a spreading volcano located within a rift caused regional fractures to bend toward the volcano in an 'hourglass' pattern (e.g. Fieale volcano in the East African Rift System; De Chabaliere and Avouac, 1994; Fig. 8d). In addition, volcanoes located on one side of a rift can capture rift fractures (e.g. axial seamount in the central segment of the Juan de Fuca Ridge in the Pacific Ocean; Johnson and Embley, 1990).

Volcanic spreading is not always related to a basal ductile layer. Volcanoes can spread by sector collapses and superficial wasting processes, even if they lack basal ductile layers (i.e. they rest upon strong, intact rocks with a high degree of internal strength; Borgia et al., 2000).

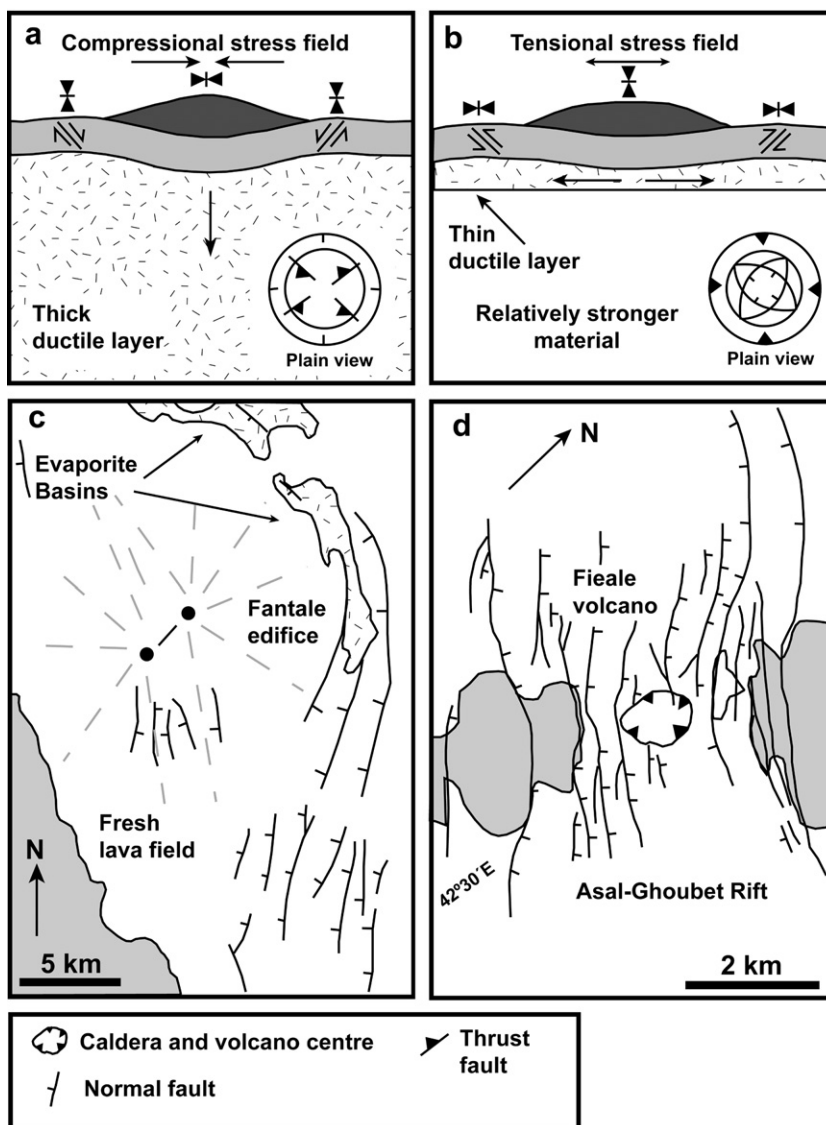


Fig. 8. Cartoons and geologic sketch maps illustrating volcanic loading, volcanic spreading and the resulting fracture patterns in areas of volcano–rift interaction (modified of van Wyk de Vries and Matela, 1998). (a) Cross-sectional view illustrating volcanic sagging (the volcano is underlain by a thick ductile layer), and a plain view of the theoretical deformational features related to the resulting local stress field (lower right corner). (b) Cross-sectional view illustrating volcanic spreading (the volcano is underlain by a thin ductile layer), and a plain view of the theoretical deformational features related to the resulting local stress field (lower right corner). (c) Fracture patterns resulting of the interplay of a sagging volcano and regional extension. Radiating gray lines indicate the extent of the volcano (e.g. Fantale volcano in the East African Rift System). (d) Fracture patterns resulting of a spreading volcano and regional extension (e.g. Fieale volcano in the East African Rift System).

4.3. The case for a ductile layer under venusian volcanoes

Volcanic spreading is favored by the presence of a thin ductile sub-volcano layer; but could such a layer exist on Venus? On Venus, the current absence of surface water (Donahue and Pollack, 1983; Grinspoon, 1993) likely precludes the existence of sedimentary layers under the volcano that might act as thin basal ductile layers. In addition, current surface modification processes and aeolian activity on Venus are orders of magnitude less than terrestrial rates, and thus not likely to contribute to the formation of sedimentary layers (Arvidson et al., 1992). Spreading in venusian volcanoes might occur, however, if a stable magmatic system exists below an individual volcano. The presence of such a magmatic system would tend to reduce the

effective viscosity of the rocks and therefore increase ductility (e.g. Borgia, 1994; van Wyk de Vries and Matela, 1998). A consequence of a stable magmatic chamber could be the existence of flowing olivine cumulates (Clague and Denlinger, 1994). On Venus rock composition, postulated from data of Venera and Vega probes together with the analysis of the volcanic landforms in the landing sites, is interpreted as tholeiitic basalt with contents in MgO wt% similar to Hawaiian lavas (e.g. Surkov, 1977; Surkov et al., 1983, 1986; Barsukov, 1992; Kargel et al., 1993). In magmas with high MgO content (e.g. Kilauea tholeiitic magma contains about 16.5 wt% MgO; Clague and Denlinger, 1994), olivine phenocrysts accumulate near the base of the reservoir. At 1100° C olivine cumulates display an ice-like rheology, with increasing system ductility related to in-

creasing intercumulus liquid (Clague and Denlinger, 1994). This particular rheology would allow cumulates to flow outward and, as such, could represent a local source for a low strength layer necessary for volcanic spreading. This mechanism is a source for local gravitational instabilities and could trigger local spreading and flank collapse (Clague and Denlinger, 1994).

A subvolcanic ductile layer could also form due to heating of the ductile lower crust, such that the strong upper crust becomes detached from the lithospheric mantle. In such a case, the ductile layer would be confined to a narrow space between the upper crust and the lithospheric mantle (McGovern, personal communication).

5. Discussion

5.1. Effect of over-pressurized magma chambers versus local gravitational stress on regional fractures

Structural mapping of volcanoes located in regional fracture systems revealed modifications in the regional fracture trend around the volcanic edifices with two resulting morphologies: (a) regional fractures bend toward the volcanic edifice (i.e. 'hourglass pattern'), as in the cases of Ne Ngam Mons, Venilia Mons, 47n198FD and 00n272SSD; and (b) regional fractures curve around the volcanic edifice (i.e. 'wristwatch pattern'), as could be the case for 21n320IV.

The modification of regional fracture trends can be explained in terms of local stress fields that result from the interaction between regional tensional stress fields and local volcano-related stress fields. As described in the previous section, the resulting fracture patterns could form in response to two different situations: (a) interaction of the regional stress fields with local stresses related to the existence of a magma chamber (i.e. uplift and dike emplacement); and (b) interaction of the regional stress field with local stresses related to volcanic loading or spreading.

Regional fractures that bend toward a volcanic construct are interpreted by McKenzie et al. (1992) to result from local stresses produced by an over-pressurized magma chamber and dike formation; in this case radial dikes align with the regional stress field away from the volcanic center and the influence of the volcano's local stress field. Radial fractures centered in the volcanic feature mark the surface manifestation of dikes (Grosfils and Head, 1994b; Ernst et al., 1995). Structural mapping of Venilia Mons, 47n198FD, 00n272SSD and 21n320IV does not reveal any evidence of radial fractures around the volcanic edifices. The absence of radial fractures can be explained if: (a) no radial dikes formed; or (b) radial dikes and associated surface fractures formed, but they were subsequently covered by volcanic flows located around the main edifice. In examples where burial of early-formed radial fractures occurs, evidence for radial fractures occurs away from the emission center and associated proximal flows (e.g. Ernst et al., 1995). In the examples analyzed herein, no evidence of embayed radial fractures is found. Radial fractures are not observed away from the edifice. The volcanic features described

herein also lack evidence of uplift, and they are much too small to be related to dynamic support (i.e. plumes); thus, the fracture patterns described herein are unlikely to result from uplift and regional extension (e.g. Cyr and Melosh, 1993). Therefore, the deflection of regional fractures around Venilia Mons, 47n198FD and 00n272SSD, might result from limited volcanic spreading and regional extension (e.g. van Wyk de Vries and Matela, 1998).

Ne Ngam Mons displays a local radial suite of fractures restricted to the eastern main edifice that ends at the base of the central edifice, and does not occur in the volcano apron (Fig. 3). The fractures lack flows at their terminations; and there is no radial arrangement of small volcanoes or pit chains that might suggest the presence of subsurface feeder dikes. An alternative explanation to the formation of these fractures is that, associated with volcano spreading, a local tensional stress field formed on the volcano main edifice (e.g. Borgia, 1994). In addition, and also associated with volcanic spreading, compressional stress is localized at the base; localization of compressive stress could be consistent with the ridges formed at the western base of the main edifice, and interpreted as local structures (Fig. 3c). The interaction of a regional tensional stress field with local stress fields related to volcanic spreading in Ne Ngam Mons could also explain the bend of the N-trending regional fractures toward the volcano and the capture of the inner part of Ajina Fossae.

Another consequence of volcanic spreading is the development of lateral flank failure processes that result in horseshoe topography (e.g. Socompa volcano; van Wyk de Vries et al., 2001). Although horseshoe topography may be associated with Ne Ngam Mons (recall lack of evidence in SAR), the absence of: (a) collapse-related deposits; (b) modification of the radial disposition of the flows due to topographic constraints; and (c) evidence of the horseshoe structure in the radar images, does not allow us to confirm the existence of lateral flank collapse for Ne Ngam Mons.

At 21n320IV concentric fractures occur around the volcanic center, and regional fractures appear to bend around the volcanic feature. This modification of the regional fracture trend could result from the interaction between a regional tensional stress field and local stress fields related to volcanic loading (Cyr and Melosh, 1993; van Wyk de Vries and Matela, 1998). Another mechanism that could explain the fracture pattern is the presence of a depression and the formation of subcircular dikes (Fig. 9a in McKenzie et al., 1992), which could result in a local stress regime that causes regional fractures to curve around the volcanic feature. The absence of a topographic depression in the area of the volcanic features leads us to favor the first option.

Study of volcano–rift interaction in the BAT region reveals that evidence of volcanic spreading in extensional environments might occur in fossae and areas of distributed regional deformation (i.e. lower strain); yet no examples for modified fracture patterns around volcanoes occur in chasmata (i.e. higher strain). The evidence of such modified fracture patterns could be covered by volcano- and chasmata-related flows. Volcanoes located in chasmata are extended without modification of re-

gional fractures (e.g. Uretsete Mons) and/or extensive flow materials bury the chasmata structures. At large topographic rises we do not observe obvious modification of the regional fracture patterns that might result from an interaction with a local stress field related to volcanic spreading. This observation could result from the relative magnitudes of the regional and local stress fields that interact. Only in cases in which regional distributed deformation or minor deformation belts (i.e. fossae) interact with a contemporaneous volcanic feature, with similar magnitudes of both regional and local volcano-related stress fields, could result in modifications of regional fracture trend. For example, in chasmata, where strain is high, the regional stress field responsible for the formation of the fractures could dominate over the local volcano-related stress field, and therefore the fracture trends would not be modified.

5.2. Volcanic spreading and modified intermediate volcanoes

Studies of the global population of large venusian volcanoes reveal little evidence of flank failure and mass wasting (McGovern and Solomon, 1997). These relations are interpreted as evidence that large venusian volcanoes are generally welded to the lithosphere (McGovern and Solomon, 1998). In contrast with large volcanoes, intermediate-size volcanoes like steep-sided domes (Pavri et al., 1992) and modified or fluted domes (Bulmer and Guest, 1996) show a wide range of flank collapse structures and debris aprons. Over 320 domes have been identified with Magellan SAR data, with more than 80% of these features showing evidence of modified morphologies (Bulmer and Guest, 1996). Two studied examples, 47n198FD and 00n272SSD, are intermediate-size volcanic edifices interpreted herein to have experienced limited volcanic spreading. Terrestrial volcanoes that are interpreted to be on a spreading phase are more susceptible to experience lateral flank failure and collapse (e.g. van Wyk de Vries and Francis, 1997). We propose that volcanic spreading in intermediate-size domes could explain the occurrence of collapse processes in domes, and that this mechanism should be considered in future studies that address tectonic modification of venusian domes.

Two of the studied examples are classified as large volcanoes: Ne Ngam Mons and Venilia Mons. However, both of these features have main edifices similar in size to the intermediate-sized volcanoes discussed herein. The general definition of large volcanoes considers main edifice size (e.g. Barsukov et al., 1986; Crumpler et al., 1997) as well as the total extent of the flow apron. Guest and Stofan (1999) and Crumpler et al. (1997) propose that some intermediate volcanoes could be large volcanoes with embayed flow aprons. If we consider the size of the main edifice, rather than the total extent of the volcanic apron, Ne Ngam and Venilia Mons are more comparable to intermediate-size volcanoes than to large volcanoes located in the highland areas. Thus, large volcanoes located in highland areas (e.g. Sif Mons) might indeed be welded to their substrates making lateral flank collapse processes difficult (McGovern and Solomon, 1998).

5.3. Nature and extent of ductile layers under venusian volcanoes

The presence of a ductile layer under the volcanic edifice can help to produce spreading (van Wyk de Vries and Matela, 1998). On Venus, subvolcanic ductile layers likely result from magmatic characteristics. Although we cannot constrain the possible thickness and lateral extent of ductile layers under the volcanoes discussed, experimental and finite element modeling on volcano spreading establish a relationship between: (a) the thickness of the ductile layer and the diameter of the cone, and (b) the angle of the deviation of the fractures toward the volcano (e.g. van Wyk de Vries and Merle, 1996; van Wyk de Vries and Matela, 1998). Unfortunately, the high material strength of venusian material as compared to terrestrial diabase (i.e. Mackwell et al., 1998) precludes using these relationships for Venus. In the case of Ne Ngam Mons, the presence of ridges at the base of the central volcanic edifice indicates that, if present, a ductile layer would be located under the main edifice. For the other examples described, only limited spreading appeared to take place; this situation is favored by the occurrence of local ductile layers related to volcano evolution. In any case, the process of volcanic spreading is favored by the presence of a thin ductile layer, although volcanoes may spread even if they lack basal ductile layers (i.e. they rest upon strong, intact rocks with a high degree of internal strength) by sector collapses and by superficial wasting processes (Borgia et al., 2000).

6. Summary and conclusions

A survey of volcano–rift locations in the BAT region identifies examples in which an interaction between regional and local volcano-related stress fields results in modification of the regional fracture trend. In the case of Ne Ngam Mons, Venilia Mons, 47n198FD and 00n272SSD modification of regional fractures in the vicinity of the volcanic edifices is interpreted to be the result of volcanic spreading and regional extension. In the case of Ne Ngam Mons, we interpret the local deformation suites (radial fractures and basal ridge) as the result of volcanic spreading. In the case of 21n320IV we interpret the local deviation of regional fractures around the volcano as a result of the influence in the regional fracture trend of the local stress field produced by the volcanic loading.

Spreading processes are favored by the presence of a subvolcanic ductile layer beneath the volcanic edifice; on Venus this layer is most likely of volcanic origin. We cannot constrain the possible thickness and lateral extent of ductile layers under venusian volcanoes, however, we suggest that the presence low strength materials is restricted to the volcano due to the limited spreading. Volcanoes can also spread by sector collapse and by superficial wasting processes if they rest upon strong, intact rocks, lack a basal decollement, and possess a high degree of internal strength (Borgia et al., 2000). Thus, volcanic spreading could be a triggering factor in flank collapse processes described for intermediate-size volcanoes on Venus. Fracture deflection only occurs in volcanoes located in fossae

and regional fractures; no examples of fracture deflection were noted in association with principal chasmata within the study area.

Acknowledgments

This work was supported by NASA Grant NAG5-13432 to V.L. Hansen and to University of Minnesota at Duluth. We thank R. Capote, M.J. Huertas, A. Marquez, O. Prieto and R. Tejero for discussions and comments of an earlier version of the manuscript. We appreciate the thorough reviews by Eric Grosfils, Ellen Stofan and Patrick McGovern that lead to a reconsideration of the initial work. This work benefited from a pre-doctoral stay at the University of Minnesota-Duluth by I. López with economic support from NASA grant NAG5-13432 and the Universidad Rey Juan Carlos mobility program.

References

- Arvidson, R.E., Greely, R., Malin, M.C., Saunders, R.S., Izenberg, N., Plaut, J.J., Stofan, E.R., Shepard, M.K., 1992. Surface modification of Venus as inferred from Magellan observations of plains. *J. Geophys. Res.* 97, 13303–13318.
- Barsukov, V.L., 1992. Venusian igneous rocks. In: Barsukov, V.L., Basilevsky, A.T., Volkov, V.P., Zharkov, V.N. (Eds.), *Venus: Geology, Geochemistry and Geophysics*. University of Arizona Press, Tucson, pp. 165–176.
- Barsukov, V.L., and 29 colleagues, 1986. The geology and geomorphology of the Venus surface as revealed by the radar images obtained by Veneras 15 and 16. In: *Proceedings of the 17th Lunar and Planetary Science Conference, Part 2*, *J. Geophys. Res.* 91, 378–398.
- Billoti, F., Suppe, J., 1999. The global distribution of wrinkle ridges on Venus. *Icarus* 139, 137–159.
- Borgia, A., 1994. The dynamic basis of volcanic spreading. *J. Geophys. Res.* 99, 17791–17804.
- Borgia, A., Delaney, P.T., Denlinger, R.P., 2000. Spreading volcanoes. *Annu. Rev. Earth Planet. Sci.* 28, 539–570.
- Bulmer, M.H., Guest, J.E., 1996. Modified volcanic domes and associated debris aprons on Venus. In: McGuire, W.J., Jones, A.P., Neuberg, J. (Eds.), *Volcano Instability on the Earth and Other Planets*. In: *Geological Society Special Publications*, vol. 110. Geological Society of London, London, pp. 349–371.
- Campbell, B.A., Arvidson, R.E., Shepard, M.K., Brackets, R.A., 1997. Remote sensing of surface processes. In: Bougher, S.W., Hunten, D.M., Phillips, R.J. (Eds.), *Venus II: Geology Geophysics, Atmosphere, and Solar Environment*. University of Arizona Press, Tucson, pp. 503–526.
- Chadwick, W.W., Howard, K.A., 1991. The pattern of circumferential and radial eruptive fissures on the volcanoes of Fernandina and Isabela. *Galapagos. Bull. Volcanol.* 53, 259–275.
- Clague, D.A., Denlinger, R.P., 1994. Role of olivine cumulates in destabilizing the flanks of Hawaiian volcanoes. *Bull. Volcanol.* 56, 425–434.
- Crisp, D., Titov, D., 1997. The thermal balance of Venus atmosphere. In: Bougher, S.W., Hunten, D.M., Phillips, R.J. (Eds.), *Venus II: Geology Geophysics, Atmosphere, and Solar Wind Environment*. University of Arizona Press, Tucson, pp. 353–384.
- Crumpler, L.S., Aubele, J.C., 2000. Volcanism on Venus. In: Sigurdsson, Houghton, H.B., McNutt, S.R., Rymer, H., Stix, J. (Eds.), *Encyclopedia of Volcanoes*. Academic Press, San Diego, CA, pp. 727–770.
- Crumpler, L.S., Head, J.W., Aubele, J.C., 1993. Relation of mayor volcanic center concentration on Venus to global tectonic patterns. *Science* 261, 591–595.
- Crumpler, L.S., Aubele, J.C., Senske, D.A., Keddie, S.T., Magee, K.P., Head, J.W., 1997. Volcanoes and centers of volcanism on Venus. In: Bougher, S.W., Hunten, D.M., Phillips, R.J. (Eds.), *Venus II: Geology Geophysics, Atmosphere, and Solar Environment*. University of Arizona Press, Tucson, pp. 697–756.
- Cyr, K.E., Melosh, H.J., 1993. Tectonic patterns and regional stresses near venusian coronae. *Icarus* 102, 175–184.
- De Chabaliere, J.-B., Avouac, J.-P., 1994. Kinematics of the Asal Rift (Djibouti) determined from the deformation of Fieale Volcano. *Science* 265, 1677–1681.
- Dieterich, J.H., 1988. Growth and persistence of Hawaiian volcanic rift zones. *J. Geophys. Res.* 93, 4258–4270.
- Donahue, T.M., Pollack, J.B., 1983. Origin and evolution of the atmosphere of Venus. In: Hunten, D.M., Colin, L., Donahue, T.M., Moroz, V.I. (Eds.), *Venus*. University of Arizona Press, Tucson, pp. 1003–1036.
- Donahue, T.M., Grinspoon, D.H., Hartle, R.E., Hodges Jr., R.R., 1997. Ion/neutral escape of hydrogen and deuterium: Evolution of water. In: Bougher, S.W., Hunten, D.M., Phillips, R.J. (Eds.), *Venus II: Geology Geophysics, Atmosphere, and Solar Wind Environment*. University of Arizona Press, Tucson, pp. 385–414.
- Ernst, R.E., Desnoyers, D.W., 2004. Lessons from Venus for understanding mantle plumes on Earth. *Phys. Earth Planet. Int.* 146, 195–229.
- Ernst, R.E., Head, J.W., Parfitt, E., Grosfils, E., Wilson, L., 1995. Giant radiating dike swarms on Earth and Venus. *Earth-Sci. Rev.* 39, 1–58.
- Ford, P.G., Pettengill, G.H., 1992. Venus topography and kilometer-scale slopes. *J. Geophys. Res.* 97, 13103–13114.
- Ford, J.P., Plaut, J.J., Weitz, C.M., Farr, T.G., Senske, D.A., Stofan, E.R., Michaels, G., Parker, T.J., 1993. *Guide to Magellan Image Interpretation*. National Aeronautics and Space Administration Jet Propulsion Laboratory Publication 93-24. 287 pp.
- Francis, P.W., Gardeweg, M., O'Callaghan, L.J., Ramirez, C.F., Rothery, D.A., 1985. Catastrophic debris avalanche deposit of Socompa volcano, north Chile. *Geology* 13, 600–603.
- Grimm, R.E., Hess, P.C., 1997. The crust of Venus. In: Bougher, S.W., Hunten, D.M., Phillips, R.J. (Eds.), *Venus II: Geology, Geophysics, Atmosphere, and Solar Environment*. University of Arizona Press, Tucson, pp. 1205–1244.
- Grindrod, P.M., Nimmo, F., Stofan, E.R., Guest, J.E., 2005. Strain at radially fractured centers on Venus. *J. Geophys. Res.* 110, doi:10.1029/2005JE002416. E12002.
- Grinspoon, D.H., 1993. Implications for the high D/H ratio for the sources of water in Venus' atmosphere. *Nature* 363, 428–431.
- Grosfils, E.B., Head, J.W., 1994a. Emplacement of a radiating dike swarm in western Vinmara Planitia, Venus: Interpretation of the regional stress field orientation and subsurface magmatic configuration. *Earth Moon Planets* 66, 153–171.
- Grosfils, E.B., Head, J.W., 1994b. The global distribution of giant radiating swarms on Venus: Implications for the global stress state. *Geophys. Res. Lett.* 21, 701–704.
- Guest, J.E., Stofan, E.R., 1999. A new view of the stratigraphic history of Venus. *Icarus* 139, 55–66.
- Guest, J.E., Bulmer, M.H., Aubele, J., Beratan, K., Greely, R., Head, J.W., Michaels, G., Weitz, C., Wiles, C., 1992. Small volcanic edifices and volcanism in the plains of Venus. *J. Geophys. Res.* 97, 15949–15966.
- Head, J.W., Crumpler, L.S., Aubele, J.C., Guest, J.E., Saunders, R.S., 1992. Venus volcanism: Classification of volcanic features and structures, associations, and global distribution from Magellan data. *J. Geophys. Res.* 97, 13153–13197.
- Iverson, R.M., 1995. Can magma-injection and groundwater forces cause massive landslides on Hawaiian volcanoes? *J. Volcanol. Geotherm. Res.* 66, 295–308.
- Johnson, P.H., Embley, R.W., 1990. Axial seamount: An active ridge axis volcano on the central Juan de Fuca Ridge. *J. Geophys. Res.* 95, 12689–12696.
- Kargel, J.S., Komatsu, G., Baker, V.R., Strom, R.G., 1993. The volcanology of Venera and VEGA landing sites and the geochemistry of Venus. *Icarus* 103, 253–275.
- Keddie, S.T., Head, J.W., 1995. Formation and evolution of volcanic edifices on the Dione Regio Rise, Venus. *J. Geophys. Res.* 100, 11729–11754.
- Kirk, R., Soderblom, L., Lee, E., 1992. Enhanced visualization for interpretation of Magellan radar data: Supplement to the Magellan special issue. *J. Geophys. Res.* 97, 16371–16380.
- Mackwell, S.J., Zimmerman, M., Kohlstedt, D.L., 1998. High-temperature deformation of diabase: Implications for tectonics on Venus. *J. Geophys. Res.* 103, 975–984.

- McGovern, P.J., Solomon, S.C., 1993. State of stress, faulting, and eruption characteristics of large volcanoes on Mars. *J. Geophys. Res.* 98, 23553–23579.
- McGovern, P.J., Solomon, S.C., 1997. Filling of flexural moats around large volcanoes on Venus: Implications for volcano structure and global magmatic flux. *J. Geophys. Res.* 102, 16303–16318.
- McGovern, P.J., Solomon, S.C., 1998. Growth of large volcanoes on Venus: Mechanical models and implications for structural evolution. *J. Geophys. Res.* 103, 11071–11101.
- McGovern, P.J., Solomon, S.C., Head, J.W., Smith, D.E., Zuber, M.T., Neumann, G.A., 2001. Extension and uplift at Alba Patera, Mars: Insights from MOLA observations and loading models. *J. Geophys. Res.* 106, 23769–23809.
- McKenzie, D., McKenzie, J.M., Saunders, R.S., 1992. Dike emplacement on Venus and on Earth. *J. Geophys. Res.* 97, 15977–15990.
- Mège, D., Cook, A.C., Garel, E., Lagabrielle, Y., Cormier, M.-H., 2003. Volcanic rifting at martian grabens. *J. Geophys. Res.* 108, doi:10.1029/2002JE001852. 5044.
- Muller, O.H., Pollard, D.D., 1977. The stress state near Spanish Peaks, Colorado determined from a dike pattern. *Pure Appl. Geophys.* 115, 69–86.
- Odé, H., 1957. Mechanical analysis of the dike pattern of the Spanish Peaks area, Colorado. *Bull. Geol. Soc. Am.* 68, 567–576.
- Pavri, B., Head, J.W., Klose, K.B., Wilson, L., 1992. Steep-sided domes on Venus: Characteristics, geologic setting, and eruption conditions from Magellan data. *J. Geophys. Res.* 97, 13445–13478.
- Siebert, L., 1984. Large volcanic debris avalanches: Characteristics of the source areas, deposits, and associated eruptions. *J. Volcanol. Geotherm. Res.* 22, 163–197.
- Stofan, E.R., Guest, J.E., Copp, D.L., 2001. Development of large volcanoes on Venus: Constraints from Sif, Gula and Kunapipi montes. *Icarus* 152, 75–95.
- Surkov, Yu.A., 1977. Geochemical studies of Venus by Venera 9 and 10 automatic interplanetary stations. *Proc. Lunar Sci. Conf.* 8, 2665–2689.
- Surkov, Yu.A., Moskal'yeva, L.P., Shcheglov, O.P., Kharyukova, V.P., Manvelyan, O.S., Kirichenko, V.S., Dudin, A.D., 1983. Determination of the elemental compositions of rocks on Venus by Venera 13 and Venera 14 (preliminary results). In: *Proc. Lunar Sci. Conf.* 13th, *J. Geophys. Res.* 88 (Supplement), A481–A493.
- Surkov, Yu.A., Moskal'yeva, L.P., Kharyukova, V.P., Dudin, A.D., Smirnov, G.G., Zaitseva, S.Ye., 1986. Venus rock composition at the Vega 2 landing site. In: *Proc. Lunar Sci. Conf.* 17th, *J. Geophys. Res.* 91, E215–E218.
- Turtle, E.P., Melosh, H.J., 1997. Stress and flexural modeling of the martian lithospheric response to Alba Patera. *Icarus* 126, 197–211.
- van Wyk de Vries, B., Francis, P.W., 1997. Catastrophic collapse at stratovolcanoes induced by gradual volcano spreading. *Nature* 387, 387–390.
- van Wyk de Vries, B., Matela, R., 1998. Styles of volcano-induced deformation: Numerical models of substratum flexure, spreading and extrusion. *J. Volcanol. Geotherm. Res.* 81, 1–18.
- van Wyk de Vries, B., Merle, O., 1996. The effect of volcano constructs on rift fault patterns. *Geology* 24, 643–646.
- van Wyk de Vries, B., Self, S., Francis, P.W., Keszthelyi, L., 2001. A gravitational spreading origin for the Socompa debris avalanche. *J. Volcanol. Geotherm. Res.* 105, 225–247.
- Watlington, R.A., Wilson, W.D., Johns, W.E., Nelson, C., 2002. Updated bathymetric survey of Kick-'em-Jenny submarine volcano. *Mar. Geophys. Res.* 23, 271–276.